Optics Communications 407 (2018) 165–168

Contents lists available at ScienceDirect

Optics Communications

journal homepage: www.elsevier.com/locate/optcom

Measurement of frequency sweep nonlinearity using atomic absorption spectroscopy

Ningfang Song, Xiangxiang Lu, Xiaobin Xu *, Xiong Pan, Wei Li, Di Hu, Jixun Liu

School of Instrumentation Science and Opto-electronics Engineering, Beihang University, Beijing 100191, China

ARTICLE INFO

Keywords:
Interferometry
Diode lasers
Frequency sweep nonlinearity
Atomic absorption spectroscopy

ABSTRACT

A novel scheme to determine frequency sweep nonlinearity using atomic saturated absorption spectroscopy is proposed and demonstrated. The frequency modulation rate is determined by directly measuring the interference fringe number and the frequency gap between two atomic transition peaks of rubidium atom. An experimental setup is established, and test results show that the frequency sweep nonlinearity is ~10%, with an average frequency modulation rate of ~1.12 THz/s. Moreover, the absolute optical frequency and optical path difference between two laser beams are simultaneously determined with this method. This low-cost technique can be used for optical frequency sweep nonlinearity correction and real-time frequency monitor.

1. Introduction

Diode lasers are widely used in scientific and civil fields ranging from wireless communication [1,2] , inverse synthetic aperture lidar detection [3,4], to atomic experiment [5–7]. However, during the frequency sweep process, undesirable nonlinearity occurs and results in significant measurement errors [8,9]. Therefore, precise measurement and feedback control of frequency sweep nonlinearity is quite important for high-precision applications.

Self-heterodyne interferometry is often used to measure frequency sweep nonlinearity [10–12]. However, radio frequency signals along with optical modulator and long fiber delay line are needed. On the other hand, wavelength meters, Fabry–Pérot etalon (FPE) or frequency comb can be used to monitor the laser frequency and measure the sweep rate of the diode laser [13–16], but the tuning of the laser must be much larger than the free spectral range of the FPE and only gives frequency information at discrete intervals. Another method uses an environmentally isolated reference interferometer to actively correct the frequency sweep nonlinearity [17–19]. Nonlinearity can also be compensated by externally triggering time domain sampling or using post-processed resampling algorithms [20,21]. However, all these measurement methods need expensive and complicated frequency reference, which limits potential application in low-cost fields.

For high-precision applications, tunable diode lasers are usually frequency locked using atomic saturated absorption spectroscopy (SAS) technique [22], which has excellent frequency stability and accuracy. In this paper, we propose and demonstrate a novel and low-cost scheme for the measurement of frequency sweep nonlinearity based on the SAS technique. This scheme has several advantages. First, this measurement can be accomplished with conventional laboratory equipment, and does not rely on expensive and bulky wavelength measurement devices to monitor the frequency, thus greatly reducing system complexity and cost. Moreover, this method enables simultaneous determination of frequency sweep rate, absolute optical frequency, and optical path difference (OPD) between two beams for one single measurement. This simple technique has potential application in fields such as frequency sweep nonlinearity correction and real-time optical frequency monitor.

2. Measurement principle

For simplicity, the period of the triangular-wave signal used to modulate the laser frequency is defined as $2T_m$. Each period is divided into two parts, the rising period and the falling period, as shown in Fig. 1. The solid curve in upper trace represents the frequency of the signal wave, the dashed curve stands for the frequency of the reference wave, the middle trace is atomic saturated absorption spectroscopy signal, and the solid curve in lower trace corresponds to the periodic beat signals. When the reference wave and the signal wave interfere, the beat signal can be written as [23]

$$I(t) = I_0\left[1 + \eta\cos\left(2\pi\alpha\tau t + 2\pi\nu_0\tau - \pi\alpha\tau^2\right)\right], \quad (1)$$

* Corresponding author.
E-mail address: xuxiaobin@buaa.edu.cn (X. Xu).

http://dx.doi.org/10.1016/j.optcom.2017.09.043
Received 3 August 2017; Received in revised form 7 September 2017; Accepted 11 September 2017
0030-4018/

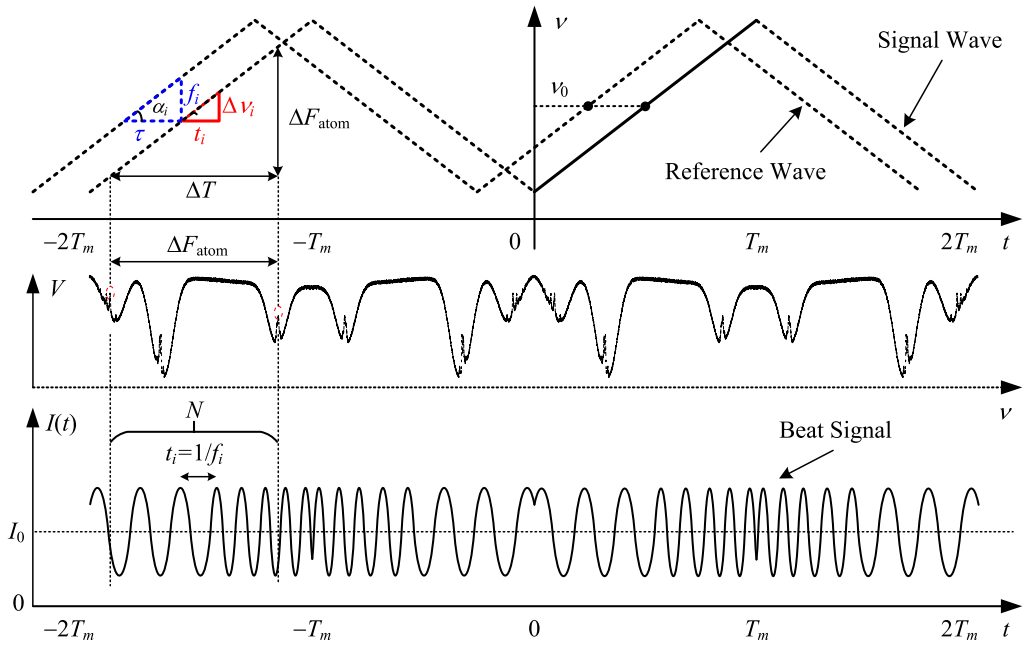

Fig. 1. (Color online). Measurement principle of the laser system: upper trace—scanning waves; middle trace—atomic SAS signal of rubidium atom, where V is the measured voltage and ν the absolute optical frequency; lower trace—beat signals.

where I_0 is the average optical intensity of the beat signal; η the interference fringe contrast; t the sweep time; α the frequency modulation rate; τ the group time delay given by $\tau = L/c$, where L is the OPD and c is the speed of light; and ν_0 the average optical frequency during the frequency sweep process. The first term in bracket of Eq. (1) represents the beat signal with the beat frequency of $\alpha\tau$, while the last two terms in bracket of Eq. (1) contribute to systematic measurement errors.

The beat frequency of the ith interference fringe can be written as

$$f_i = \alpha_i \times \tau \quad (i = 1, 2, \ldots, N), \tag{2}$$

where N is the fringe number, $\Delta T(\Delta T < T_m)$ the sweep time corresponding to two transition peaks in Fig. 1, and α_i the frequency modulation rate during time interval t_i. If N is large enough, it is reasonable to assume that the modulation rate is constant for each time interval t_i with the relation $\sum_{i=1}^{i=N} t_i = \Delta T$. On the other hand, for each time interval t_i, the optical frequency increases by $\Delta\nu_i = \alpha_i \times t_i$. By adding each minor frequency increment during ΔT yields $\sum_{i=1}^{i=N} \Delta\nu_i = \Delta F_{atom}$, where ΔF_{atom} is the fixed frequency gap of the two transition peaks of alkali atoms. Note that for certain atoms, ΔF_{atom} is a constant value and can be precisely known. This typical value is on the order of GHz and immune to environmental perturbations.

The fringe number N of the beat signal is measured with peak finding algorithms, and each beat frequency can be determined using the atomic peak location related scanned time. Consequently, the frequency modulation rate and absolute optical frequency can be calculated as:

$$\begin{aligned} \alpha_i &= f_i \times \Delta F_{atom}/N \\ \nu_i &= \nu_0 + i \times \Delta F_{atom}/N. \end{aligned} \tag{3}$$

Furthermore, the delay time and OPD can also be determined as follows:

$$\begin{aligned} \tau &= N/\Delta F_{atom} \\ L &= cN/\Delta F_{atom}. \end{aligned} \tag{4}$$

The spatial OPD resolution is $\Delta L = c/\Delta F_{atom}$, consistent with that reported in [21]. As can be seen from Eqs. (3) and (4), measurement resolution of the modulation rate and absolute optical frequency is inversely proportional to the fiber delay length (fringe number), while resolution of the OPD is constant regardless of the fiber delay length. Therefore, when measuring the modulation rate and absolute optical frequency, a shorter fiber length is preferred in low-precision and small-size applications and vice versa. To further increase the OPD resolution, larger scanned frequency range is a good option. For experimental plans aim at OPD determination, fiber length of several meters long is enough to achieve ~ cm resolution.

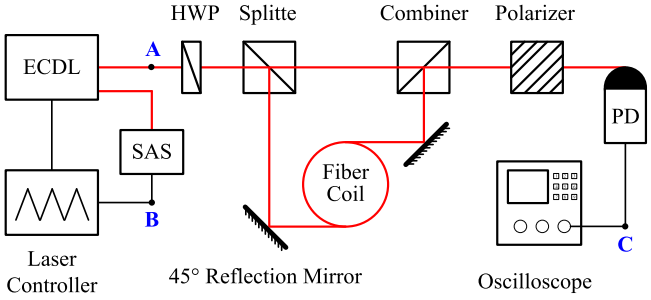

Fig. 2. (Color online). Schematic of experimental apparatus: red line—optical signal; black line—electronic signal. The points B, and C represent measurement locations of atomic SAS signal and beat signal respectively, while frequency modulation rate and absolute optical frequency at point A are calculated based on measured data at points B and C.

3. Experimental setup and results

According to the measurement principle described in Section 2, schematic of the experimental apparatus is depicted in Fig. 2 to measure the frequency sweep nonlinearity. The tunable laser is an external cavity diode laser (ECDL, Toptica DL Pro) operating at 780.24 nm, which corresponds to resonant transitions of rubidium (Rb) atom. In principle, any two of the transition peaks can be used as an absolute frequency reference, and two transitions of $5S_{1/2}F = 2 \rightarrow 5P_{3/2}F' = 2, 3$ crossover and $5S_{1/2}F = 2 \rightarrow 5P_{3/2}F' = 3$ (the scanned frequency range ΔF_{atom} is 4.235 GHz) is used in this experiment, where F and F' denote the ground state and excited state, respectively. The laser frequency is modulated with a triangular wave by driving the piezoelectric transducer (PZT) with a repetition rate of 100 Hz and a peak-to-peak sweep voltage of 13 V, corresponding to an overall scanned frequency range of 5.666 GHz.

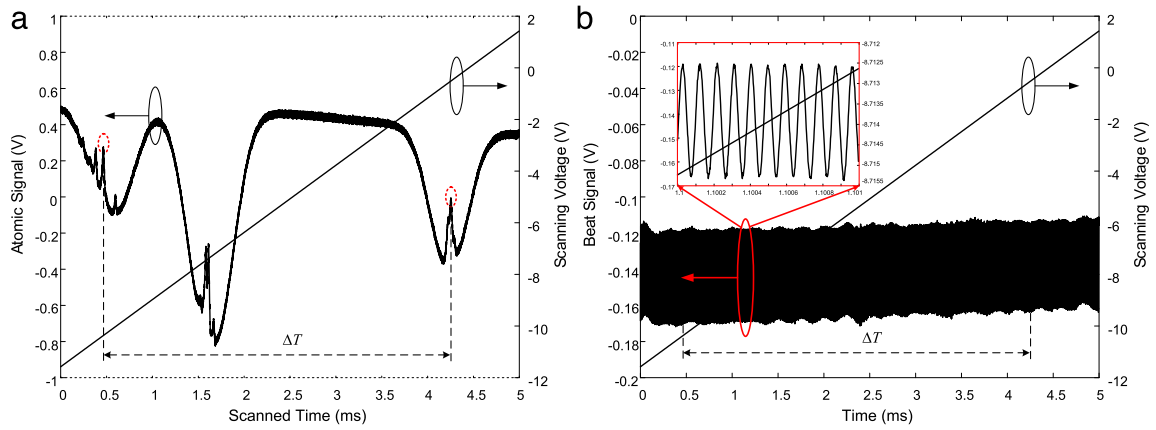

Fig. 3. (Color online). Experimental results: (a) atomic signal obtained at point B in Fig. 2 and (b) beat signal obtained at point C in Fig. 2. The inset shows about 11 interference fringes.

The laser frequency is modulated with a triangular wave from the laser controller, and the average frequency is chosen to be around the atomic transition lines. The ECDL output light is split into two beams by utilizing a half-wave plate (HWP) and splitter. A polarization maintaining (PM) fiber coil is used as the optical time delay. The two beams are recombined by the combiner and linearly polarized by a polarizer. The beat signal is received by a high-speed photodetector (PD, Newport 1554B), and the converted electronic signal (70 mV for each beam) is sent to an oscilloscope (Tektronix MDO3104) for real-time signal acquisition and analysis. The sampling rate is set 500 MS/s (million samples per second) with a total data acquisition length of 10 MS and an overall sampling time of 20 ms.

The experimental results are shown in Fig. 3, with atomic SAS signal in Fig. 3(a) and beat signal in Fig. 3(b). The time interval ΔT is determined to be ~3.79 ms, corresponding to the two peaks of atomic signal (red elliptical circle with dotted-line) in Fig. 3(a), with an uncertainty of ±0.2 μs. The fringe number N is 42,120 ± 100 by using peak finding algorithms. Periodic fringes can be observed from the inset (red box) in Fig. 3(b).

The frequency modulation rate (measured at point A in Fig. 2) is calculated from Eq. (3), which is shown in Fig. 4. The frequency modulation rate is determined to be ~1.12±0.11 THz/s, which means a frequency sweep nonlinearity of ~10% and an average modulation rate of 1.12 THz/s. As expected, the frequency modulation rate is not constant, but shows a weak linear relationship with scanned time. Furthermore, clear oscillations of the frequency modulation rate are visible, consistent with that reported in [24]. One point to be particularly mentioned is that the frequency modulation rate over entire rising period and falling period can be calculated using this technique.

Verifications with a commercial wavelength meter are hardly feasible, because the highest sampling rate of the wavelength meter is ~33 samples per second, which is much smaller than the sampling rate used in our experiment (500 MS/s). Instead, we use an alternative way to validate measured sweep nonlinearity. According to Eqs. (3) and (4), the modulation rate, absolute optical frequency and the OPD are both calculated based on the delay time, which means these parameters have similar measurement precision. Therefore, measurement result of frequency sweep nonlinearity can be indirectly validated by checking the OPD.

Based on Eq. (4), the OPD (delay time) is calculated to be 2981.484 ± 7.08 m (9.945 ± 0.16 μs), which is in good agreement with the true OPD (delay time) of 3028.9 ± 0.01 m (10.1 μs), which is obtained by a high-precision optical backscattering reflectometer (OBR). Therefore, the measurement error of OPD is calculated to be 0.2%, which indicates that the measurement error of frequency sweep nonlinearity is 0.2%. This measurement error of 0.2% is mainly due to the fringe number uncertainty ΔN, which essentially resulted from the ambiguity of precisely located scanned time. The scanned time corresponds to atomic transition

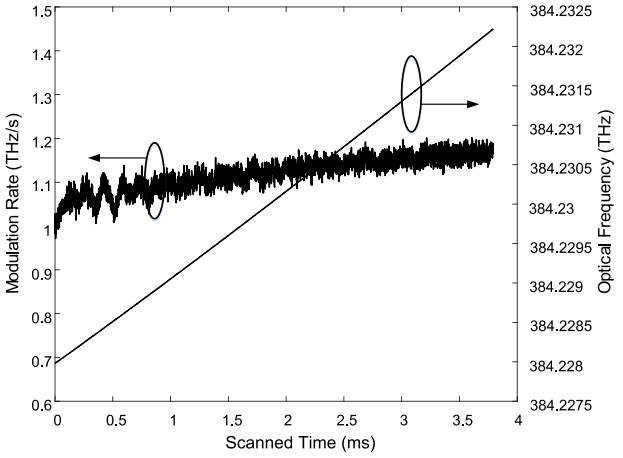

Fig. 4. Measured frequency modulation rate and absolute optical frequency over scanned time.

peak locations. Under experimental conditions, the spatial OPD (delay time) resolution ΔL ($\Delta\tau$) is calculated to be 7 cm (0.236 ns).

Moreover, this method can also be used to simultaneously measure the absolute optical frequency and OPD for one single run. The absolute optical frequency changes from 384.228 to 384.2323 THz with a frequency resolution of 100 kHz in the 3.8 ms scanned time. It seems linear frequency tuning, but essentially, contains small frequency fluctuation. This high-frequency resolution is comparable to that of conventional wavelength meters. The optical frequency resolution can be set to 100 MHz with a short fiber length of only 2 m, which indicates potentially portable application for field frequency monitor.

4. Discussion

The frequency sweep nonlinearity arises from several reasons. First, the measurement is affected by vibration and airflow fluctuation. According to [24], drifts and vibrations occurring along the optical path will be magnified by a factor of $\Omega = \nu_0/\Delta\nu$ (~9×10^4) in this experiment. Therefore, small vibrations and drift errors can result in significant effects. On the other hand, optical path variation of dispersive elements introduces change on the delay time (positively proportional to the fringe number), and measurement errors in determining the modulation rate as well as optical frequency. From Eqs. (3) and (4), both the modulation rate and absolute optical frequency are inversely proportional to the delay time. This essential relationship does induce frequency sweep nonlinearity in principle. Moreover, direct modulation

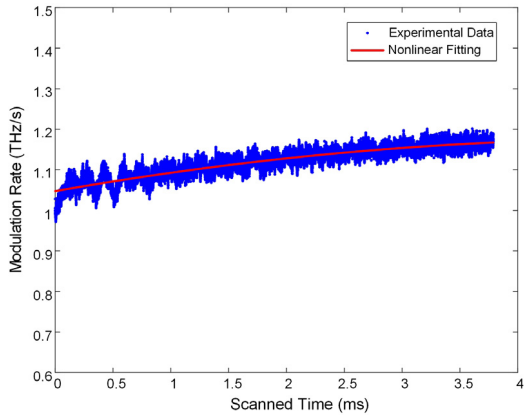

Fig. 5. (Color online). Nonlinear fitting of the frequency modulation rate over scanned time.

of the laser cavity with a triangular wave also induces frequency sweep nonlinearity, which is due to the fact that the laser frequency is inversely proportional to the cavity length. Therefore, even a linear sweep of the laser cavity can still result in nonlinearity of the frequency sweep.

To get a more straightforward knowledge on the frequency sweep nonlinearity, a second-order polynomial fitting of the modulation rate over scanned time is performed, as illustrated in Fig. 5. The goodness of this nonlinear fitting is 91%. The fitting can be expressed as $\alpha(t) = \alpha_2 t^2 + \alpha_1 t + \alpha_0$, where $\alpha(t)$ is the measured chirp rate. After some calculations, the corresponding frequency tuning coefficients are determined to be $\alpha_2 = -5.779 \pm 0.114$ GHz/s^3, $\alpha_1 = 34.16 \pm 0.105$ GHz/s^2, and $\alpha_0 = 1.126$ THz/s, respectively. The former two terms represent the third and second order frequency modulation of the frequency sweep process. The fitting results are consistent with that of [25].

The technique, which is based on atomic saturated absorption spectroscopy, enables simultaneous measurement of the frequency modulation rate and its nonlinearity, OPD, and absolute optical frequency. All these measurements are based on routine laboratory equipment and no bulky or expensive wavelength meters are needed, greatly reducing system complexity and cost.

5. Conclusion

In this paper, a novel and low-cost scheme to measure the frequency sweep nonlinearity is proposed and demonstrated. The operation principle of using atomic saturated absorption spectroscopy to determine the frequency modulation rate and the sweep nonlinearity is presented. By measuring the interference fringe number and the frequency gap of atomic transition peaks of Rb atom, the frequency modulation rate is determined to be 1.12±0.11 THz/s with a nonlinearity of 10%. This technique enables simultaneous measurement of OPD with an uncertainty of ±0.2% and a spatial resolution of 7 cm. The absolute optical frequency is also monitored with a frequency resolution of 100 kHz. Unlike conventional methods to determine the sweep nonlinearity, this approach needs no expensive or bulky wavelength meters as the frequency reference and can be implemented with routine laboratory equipment, thus greatly reducing system complexity and cost. This technique has potential applications in fields such as optical frequency sweep nonlinearity correction and potable real-time frequency monitor.

Acknowledgments

This work was supported by Major Instrument Project of China Ministry of Science and Technology under grant No. 2013YQ040877. The authors would like to thank Fuyu Gao and Haoshi Zhang for helping to calibrate the fiber coil length and Wei Cai for useful discussions.

References

[1] F. Feng, H. Page, R.V. Penty, I.H. White, Free space optical wireless communications using directly modulated two-electrode high brightness tapered laser diode, Electron. Lett. 48 (2012) 281–283.
[2] J. Xu, M. Kong, A. Lin, Y. Song, J. Han, Z. Xu, B. Wu, S. Gao, N. Deng, Directly modulated green-light diode-pumped solid-state laser for underwater wireless optical communication, Opt. Lett. 42 (2017) 1664–1667.
[3] H. Zhou, B. Nemati, M. Shao, C. Zhai, I. Habn, W. Schelze, R. Trahan, Low-cost chirp linearization for long range ISAL imaging application, Proc. SPIE 9846 (2016) 98460D.
[4] A. Kohl, C. Canal, A. Laugustin, O. Rabot, Disruptive laser diode source for embedded LIDAR sensors, Proc. SPIE 10086 (2017) 100860V.
[5] C.E. Wieman, L. Hollberg, Using diode laser for atomic physics, Rev. Sci. Instrum. 62 (1991) 1–20.
[6] E.C. Cook, P.J. Martin, T.L. Brown-Heft, J.C. Garman, D.A. Steck, High passive-stability diode-laser design for use in atomic-physics experiments, Rev. Sci. Instrum. 83 (2012) 043101.
[7] C. Kurbis, A. Bawamia, M. Kruger, R. Smol, A. Wicht, A. Peters, G. Trankle, Micro-integrated extended cavity diode lasers for precision potassium spectroscopy in space, Opt. Express 22 (2012) 7790–7798.
[8] R.E. Saperstein, N. Alic, S. Zamek, K. Ikeda, B. Slutsky, Y. Fainman, Processing advantages of linear chirped fiber bragg gratings in the time domain realization of optical frequency-domain reflectometry, Opt. Express 15 (2007) 15464–15479.
[9] M.U. Piracha, D. Nguyen, D. Mandridis, T. Yilmaz, I. Ozdur, S. Ozharar, P.J. Delfyett, Range resolved lidar for long distance ranging with sub-millimeter resolution, Opt. Express 18 (2010) 7184–7189.
[10] B. Boggs, C. Greiner, T. Wang, H. Lin, T.W. Mossberg, Simple high-coherence rapidly tunable external-cavity diode laser, Opt. Lett. 23 (1998) 1906–1908.
[11] C.J. Karlsson, F.A.A. Olsson, Linearization of the frequency sweep of a frequency-modulated continuous-wave semiconductor laser radar and the resulting range performance, Appl. Opt. 38 (1999) 3376–3386.
[12] K. Nakamura, T. Miyahara, H. Ito, Observation of a highly phase-correlated chirped frequency comb output from a frequency-shifted feedback laser, Appl. Phys. Lett. 72 (1998) 2631–2633.
[13] O. Kazharsky, S. Pakhomov, A. Grachev, Y. Mironov, I. Goncharov, A. Matveev, Broad continuous frequency tuning of a diode laser with an external cavity, Opt. Commun. 137 (1997) 77–82.
[14] P. Del'Haye, O. Arcizet, M.L. Gorodetsky, R. Holzwarth, T.J. Kippenberg, Frequency comb assisted diode laser spectroscopy for measurement of microcavity dispersion, Nat. Photon. 3 (2009) 529–533.
[15] F.R. Giorgetta, I. Coddington, E. Baumann, W.C. Swann, N.R. Newbury, Fast high-resolution spectroscopy of dynamic continuous-wave laser sources, Nat. Photon. 4 (2010) 853–857.
[16] E. Baumann, F.R. Giorgetta, I. Coddington, L.C. Sinclair, K. Knabe, W.C. Swann, N.R. Newbury, Comb-calibrated frequency-modulated continuous-wave ladar for absolute distance measurements, Opt. Lett. 38 (2013) 2026–2028.
[17] G. Gorju, A. Jucha, A. Jain, V. Crozatier, I. Lorgere, J.-L.L. Gout, F. Bretenaker, Active stabilization of a rapidly chirped laser by an optoelectronic digital servo-loop control, Opt. Lett. 32 (2007) 484–486.
[18] N. Satyan, A. Vasilyev, G. Rakuljic, V. Leyva, A. Yariv, Precise control of broadband frequency chirps using optoelectronic feedback, Opt. Express 17 (2009) 15991–15999.
[19] Z.W. Barber, W.R. Babbitt, B. Kaylor, R.R. Reibel, P.A. Roos, Accuracy of active chirp linearization for broadband frequency modulated continuous wave ladar, Appl. Opt. 49 (2010) 212–219.
[20] E.D. Moore, R.R. McLeod, Correction of sampling errors due to laser tuning rate fluctuations in swept-wavelength interferometry, Opt. Express 16 (2008) 13139–13149.
[21] P.A. Roos, R.R. Reibel, T. Berg, B. Kaylor, Z.W. Barber, W.R. Babbitt, Ultrabroadband optical chirp linearization for precision metrological applications, Opt. Lett. 34 (2009) 3692–3694.
[22] Paul Siddons, Charles S. Adams, Chang Ge, Ifan G. Hughes, Absolute absorption on rubidium D lines: comparison between theory and experiment, J. Phys. B: At. Mol. Opt. Phys. 41 (2008) 155004.
[23] J. Zheng, Analysis of optical frequency-modulated continuous-wave interference, Appl. Opt. 43 (2004) 4189–4198.
[24] H.J. Yang, J. Deibel, S. Nyberg, K. Riles, High-precision absolute distance and vibration measurement with frequency scanned interferometry, Appl. Opt. 44 (2005) 3937–3944.
[25] T.J. Ahn, D.Y. Kim, Analysis of nonlinear frequency sweep in high-speed tunable laser sources using a self-homodyne measurement and Hilbert transformation, Appl. Opt. 46 (2007) 2394–2400.